

# Role of Ocular Complement Factor H in a Murine Model of Choroidal Neovascularization

Valeriy V. Lyzogubov, Ruslana G. Tytarenko, Purushottam Jha, Juan Liu, Nalini S. Bora, and Puran S. Bora

From the Department of Ophthalmology, Jones Eye Institute, Pat & Willard Walker Eye Research Center, University of Arkansas for Medical Sciences, Little Rock, Arkansas

**The objective of this study was to explore the relationship between local (ie, ocular) complement factor H (CFH) and choroidal neovascularization (CNV) associated with wet age-related macular degeneration (AMD), a leading cause of irreversible blindness, in laser-treated C57BL/6 mice. Immunohistochemical and RT-PCR analysis of retinal pigmented epithelium (RPE)-choroid sclera revealed that the expression of CFH was down-regulated on day 1 with a dramatic increase on days 5 and 7 postlaser injury. Flat mount and Western blot analysis further revealed that membrane attack complex (MAC) expression was up-regulated on days 1 and 3 postlaser injury; however, MAC was down-regulated on days 5 and 7 postinjury but was still higher than in non-injured mice. Similar patterns for CFH and MAC were observed for RPE cells when serial paraffin sections of the laser spots were analyzed. Subretinal injection of siRNA directed against CFH resulted in a threefold suppression of CFH in the RPE and choroid without affecting either CFH levels in the liver or the functional activity of the alternative pathway in the peripheral blood. Ocular knock-down of CFH resulted in increased MAC deposition, which leads to the early onset as well as exacerbation of laser-induced CNV. In conclusion, our findings provide evidence that CFH present on RPE and choroid regulates local MAC formation that is critical for the development of laser-induced CNV. (*Am J Pathol* 2010, 177:1870–1880; DOI: 10.2353/ajpath.2010.091168)**

Age-related macular degeneration (AMD) is the leading cause of irreversible blindness among individuals over the age of 50 worldwide. Approximately two million people in the United States alone have AMD, and it is projected that by 2020, approximately three million people

will develop this disease.<sup>1,2</sup> In AMD there is a progressive destruction of the macula leading to the loss of central vision. Two major clinical phenotypes of AMD are recognized—a non-exudative (dry type, 85% of the cases), and an exudative (wet type, 15% of the cases). Although the dry form of AMD is more prevalent, catastrophic vision loss is more frequently associated with the wet form, specifically from the complication of choroidal neovascularization (CNV).<sup>2–8</sup> Two major aspects of AMD may influence severity of the disease: new vessel growth and retinal pigmented epithelium (RPE) degeneration, which leads to the break-down of blood-retinal barrier. Affected retinal nutrition due to the RPE cell loss and uncontrolled vascular growth with leakage and retinal detachment predispose to photoreceptors loss and blindness.<sup>2,8</sup>

An accelerated and reliable way to produce CNV in animals is to rupture Bruch's membrane with laser photocoagulation.<sup>4,5,9</sup> CNV induced in rodents by this method is useful to gain insights into the pathogenesis of new vessel growth from the choroid and has been remarkably successful in predicting potential points of therapeutic interventions.<sup>4,5,9</sup> There is a substantial body of evidence implicating complement in AMD both in humans and in experimental animals.<sup>2,4,5,10–13</sup> Complement components, complement activation products and complement regulatory proteins have been localized in drusen in patients with AMD and during the course of laser-induced CNV in rodents.<sup>2,11–12</sup> The formation of membrane attack complex (MAC) due to local complement activation was reported to be central to the development of laser-induced CNV in mice.<sup>4,5,14</sup> We have

---

Supported by National Institutes of Health (NIH) grants EY014623 and EY016205, and grants from University of Arkansas for Medical Sciences, Little Rock, AR. The use of the facilities in the University of Arkansas for Medical Sciences Digital and Confocal Microscopy Laboratory was supported by NIH grant 2P20 RR16460 and NIH/National Center for Research Resources grant 1 S10 RR 19395.

Accepted for publication June 24, 2010.

Supplemental material for this article can be found on <http://ajp.amjpathol.org>.

Address reprint requests to Nalini S. Bora, Ph.D., or Puran S. Bora, Ph.D., Department of Ophthalmology, Jones Eye Institute, 4301 West Markham, Mail slot 523, Little Rock, AR 72205. E-mail: nbora@uams.edu or pbora@uams.edu.

previously reported that MAC formation via the alternative pathway activation, but not the classical or lectin pathway, was essential for the release of growth factors that drive the development of laser-induced CNV in mice.<sup>4,15</sup> Our results also indicated that the alternative pathway activation was due to the reduced expression of regulatory protein—complement factor H (CFH).<sup>15</sup>

CFH, a 155-kDa glycoprotein is the key regulator of the alternative pathway of complement activation.<sup>16,17</sup> CFH is present in soluble form in plasma and fluid phase and may bind to the surface of host cells and biological surfaces.<sup>16</sup> CFH has been reported to be present in human and mouse ocular tissues such as RPE and choroid and is associated with drusen in AMD patients.<sup>12,18,19–21</sup> However, to our knowledge, the role of ocular CFH in the regulation of local complement system in wet AMD has not been explored yet. This study was undertaken to investigate the role of ocular CFH in the development of laser induced CNV in mice. Our results suggest that local inhibition of the alternative pathway of complement activation may be used as a therapeutic tool in the treatment of wet AMD in future.

## Materials and Methods

### Animals

Male C57BL/6 mice (7–9 weeks old) were purchased from the Jackson Laboratory (Bar Harbor, ME). This study was approved by the Institutional Animal Care and Use Committee (IACUC), University of Arkansas for Medical Sciences, Little Rock, AR.

### Induction of CNV

CNV was induced by laser-photocoagulation in C57BL/6 mice with an argon laser (Lumenis Inc., Santa Clara, CA) as previously described.<sup>3,9,15,22</sup> Three laser spots (50  $\mu$ m spot size, 0.05 seconds duration, 260 mW power) were placed in each eye close to the optic nerve. Production of a vaporization bubble at the time of laser confirmed the rupture of Bruch's membrane.

### Measurement of CNV

Animals were perfused with 0.75 ml of phosphate-buffered saline (PBS) containing 50 mg/ml of fluorescein-labeled dextran (FITC-Dextran, 2 million average mw, Sigma, St. Louis, MO) before they were sacrificed. The eyes were harvested, fixed for 4 hours in 10% phosphate-buffered formalin (Sigma, St. Louis, MO), and RPE-choroid-sclera flat mounts were prepared.<sup>9,15,22</sup> The flat mounts were mounted in ProLong Antifade reagent (Invitrogen, Carlsbad, CA) with the sclera facing down, examined under a ZEISS LSM 510 laser confocal microscope, and images of laser spots were captured. Area of green fluorescence (CNV size) was measured using ImageJ program (National Institute of Health, Bethesda, MD). The green color in the laser spot represents CNV complex. If the CNV was <3% of the total laser spot area,

it was graded as negative, whereas CNV >3% was considered positive.

### Immunohistochemistry

Naïve (nonlasered) and laser treated animals were sacrificed at day 1, 3, 5, and 7 postlaser ( $n = 10$  mice per time point). The eyes were harvested and fixed for 4 hours in 10% phosphate-buffered formalin (Sigma, St. Louis, MO). One set of samples ( $n = 10$  eyes per time point) was processed for RPE-choroid-sclera flat mounts.<sup>9,15,22</sup> Another set of samples ( $n = 10$  eyes per time point) was arranged in composite blocks (2 eyes from each group) and embedded in paraffin. Serial sections were prepared<sup>23</sup> to find laser-injured area. Two close sections (10 eyes in each section) were placed on each slide. One section was used for immunohistochemical staining, and another section was used as a control. All samples were processed at the same time and in the same manner. Sheep polyclonal antibody to CFH (Lot # ab8842, Abcam, Cambridge, MA) and rabbit polyclonal antibody reactive with mouse C9 (kindly provided by Prof. B.P. Morgan, University of Wales College of Medicine, Cardiff, UK) were used to stain CFH and MAC, respectively. FITC-conjugated AffiniPure donkey anti-sheep IgG (H+L) (Lot # 72193, Jackson Immuno-research laboratories, West Grove, PA), AF (Alexa Fluor) 594-conjugated donkey anti-sheep IgG (H+L), AF594-conjugated goat anti-rabbit IgG (H+L) (Lot # 536045 and # 561784, respectively, all from Molecular Probes, Eugene, OR) were used as the secondary antibody. To block nonspecific binding tissues were incubated in 5% bovine serum albumin (BSA) (Fisher Scientific, Fair Lawn, NJ) prepared on 0.05 mol/L (pH = 7.4) PBS (Invitrogen, Grand Island, NY) for 2 hours at +25°C. Primary antibody was diluted in 1% BSA (anti-CFH antibody - 1:200 and anti-MAC - 1:4000) and was applied for 12 hours at +4°C and then secondary antibody (all diluted 1:400) was used for 1 hour at +25°C. Samples were washed with PBS three times for 10 minutes, between each changes of antibody. Control stains were performed with isotype-matched control antibodies at concentrations similar to those of the primary antibodies and staining by omission of the primary or secondary antibodies. To block autofluorescence samples were treated with 1% Sudan Black B (Fisher Scientific, Fair Lawn, NJ) as previously described.<sup>24</sup>

Flat mounts were stained for CFH and MAC and Z-stack images (1  $\mu$ m thickness of each optical section, seven optical sections in one Z-stack) of laser-injured area were captured using ZEISS LSM 510 laser confocal microscope set up with Beam Splitters as follows: 488 nm laser (25%) window 505–550 nm, 561 nm laser (25%) window 575–615 nm. Eight-bit images were obtained using the microscope in sequential mode with line average of four and format 1024  $\times$  1024 pixels. We used Plan-Apochromat 20 $\times$ /0.8 objective. Mean intensity (mean gray value, within range from 0 to 255) of green and red fluorescence in area of laser injury was measured using ImageJ program (National Institute of Health,

Bethesda, MD) in each Z-stack layer. Mean value of intensity for each laser spot was calculated. Experiment was repeated three times with similar results.

Paraffin-embedded sections with laser injured areas were used for immunohistochemical staining (IHC) for CFH and MAC. IHC procedure was done as described above for flat mounts; antigen unmasking solution (Vector Laboratories, Burlingame, CA) was used to retrieve antigens. After IHC the sections were treated with 1% Sudan Black B and mounted in ProLong Antifade reagent. Laser injured areas on paraffin sections were captured as images of differential interference contrast (DIC), green (CFH), and red (MAC) fluorescence in one single plane (1- $\mu$ m optical slice). We used Plan-Apochromat 63 $\times$ /1.4 objective and Immersol 518 F oil (ne = 1.518 [23°C] Carl Zeiss, Oberkochen, Germany). DIC was used to identify different structures. Experiment was repeated 3 times with similar results.

### Small Interfering RNA Synthesis and Administration

Small interfering RNA (siRNA) was used to knock-down CFH gene *in vivo*. Three target sequences were identified at different locations within the coding region of mouse CFH gene,<sup>25</sup> and siRNAs were designed corresponding to those sequences. Control siRNAs were randomly scrambled sequences with minimum or no homology with the siRNA as well as target sequence and were synthesized at Invitrogen. siRNAs were generated by the BLOCK-iT RNAi Designer software (Invitrogen). siRNAs (duplexes of sense and anti-sense strands) were 25-nucleotides long double-stranded RNAs. Sense and anti-sense strands of siRNAs in 5'-3' direction were: CFH (GenBank Accession no. NM\_009888): CFH-1 (sense): 5'-CAGGCUCGUGGUCAGAACAACUAUA-3', (antisense): 5'-UAUAGUUGUUCUGACACGAGCCUG-3'; CFH-2 (sense): 5'-GGACAUGGGUCAGUUUCUUGCAUUA-3'; (antisense): 5'-UAAUGCAAGAAACUGACCCAU-3'; CFH-3 (sense): 5'-CAGGAGUACGAACGCUCAAUCUGUA-3'; (antisense): 5'-UACAGAUUGAGCGUUCGUACUCCUG-3'; Control -1 (sense): 5'-CAGUGCUCUGGAAGACAACUCGAUA-3', (antisense): 5'-UAUCGAGUUGUCUCCAGAGCACUG-3'; Control -2 (sense): 5'-GGAGGGUGACUCUUUCGUUAACUUA-3', (antisense): 5'-UAAGUUAACGAAAGAGUCACCCUCC-3'; Control -3 (sense): 5'-CAGCAUGCAAGCUCGCUAAUAGGUA-3', (antisense): 5'-UACCUAUUAGCGAGCUUGCAUGCUG-3'. Lipid-based *in vivo* transfection reagent (Altogen Biosystems, Las Vegas, NV) was used as the vehicle for delivery of siRNAs and two different doses (20 pM and 80 pM) of CFH siRNA were tested. Mice were divided into 3 groups—group 1 ( $n = 20$  mice) received single subretinal injection of CFH siRNAs (equal mixture of all 3 CFH siRNAs in 2  $\mu$ l), group 2 ( $n = 20$  mice) received control siRNAs (equal mixture of all 3 control siRNAs in 2  $\mu$ l), and group 3 ( $n = 20$  mice) was injected with 2  $\mu$ l of vehicle (lipid-based *in vivo* transfection reagent). Injections were performed within 3–5 minutes after laser treatment in region close to laser injured area under microscope. Mice were injected at the day of laser treatment (day 0) and were sacrificed at day 1, 3, 5,

and 7 postlaser. Eyes were harvested and RPE-choroid tissue was used for total RNA and total protein extraction. Assessment of CFH suppression was done by semiquantitative RT-PCR and semiquantitative Western blot analysis described below. Experiment was repeated three times with similar results.

### Localization of CFH siRNA

For localization study above mentioned siRNAs modified with Alexa 488 (AF488, green fluorescence) were used. Mice were divided into three groups—group 1 ( $n = 12$  mice) received single subretinal injection of CFH AF488 siRNA (equal mixture of all 3 siRNAs with total concentration of siRNA 1  $\mu$ g/ $\mu$ L or 80 pM in 2  $\mu$ l) and group 2 ( $n = 12$  mice) received control AF488 siRNA (equal mixture of all 3 with total concentration of siRNA 1  $\mu$ g/ $\mu$ L or 80 pM in 2  $\mu$ l). Mice were injected at the day of laser treatment (day 0) and were sacrificed at day 1, 3, 5, and 7 postlaser. Group 3 had naïve mice ( $n = 6$  mice) which served as the control. Eyes were harvested and fixed in formalin and divided into two sets. One set of eyes (three eyes per each time point) was processed for RPE-choroid-sclera flat mounts, and the flat mounts were stained for CFH (AF594-conjugated donkey anti-sheep IgG [H+L] were used as secondary Abs). Another set of eyes (three eyes per each time point) were used to cut serial paraffin sections (5  $\mu$ m thick) and examined without any additional staining.

### Semiquantitative RT-PCR Analysis

Total RNA was extracted from pooled RPE-choroid tissue and liver for RT-PCR using the RNeasy Kit (Qiagen, Valencia, CA). Specific oligonucleotide primers derived from mouse CFH gene<sup>25</sup> were synthesized at Integrated DNA Technologies, Inc. (Coralville, IA). RT-PCR was conducted using the following primers:  $\beta$ -actin (746 bp) forward: 5'-GCCACCAGTTCGCCATGGATGA-3', reverse: 5'-GTCAGGCAGCTCATAGCTCTTC-3'; CFH (840 bp) forward: 5'-TTGGAATTCTCCTGCCATTC-3', reverse: 5'-ACCTTCCATCTTTGCACACC-3'. RT-PCR for CFH and  $\beta$ -actin transcripts was performed using 0.1  $\mu$ g of total RNA as template and the reagents purchased from Applied Biosystems (Foster City, CA). PCR was performed using 25 and 30 cycles. The negative controls included sterile water instead of the RNA and a reaction without reverse transcriptase. RT-PCR products were analyzed on 1% agarose gel and quantitated by densitometry using Quantity one 4.2.0 (Bio-Rad). Experiment was repeated three times with similar results.

### Semiquantitative Western Blot Analysis

Total protein was extracted from pooled RPE-choroid tissue and liver. The tissue was homogenized and solubilized in ice-cold PBS containing protease inhibitors as previously described.<sup>4,15</sup> Briefly, electrophoresis was performed on 7.5% SDS-PAGE slab gel and the separated proteins were transferred to polyvinylidene difluo-

ride (PVDF) membranes. The blots were blocked with 5% nonfat dry milk. Sheep polyclonal anti-CFH from Abcam (Lot # ab8842, Cambridge, MA) and rabbit polyclonal anti-C9 (kindly provided by Prof. B.P. Morgan, University of Wales College of Medicine, Cardiff, UK) was used as the primary antibodies, and the blots were treated separately with these antibodies overnight at +4°C. In past, we have used rabbit polyclonal anti-C9 to stain MAC in mouse eye.<sup>4,15</sup> This antibody recognizes neo-epitopes on C9 in MAC complex. Control blots were reacted with equivalent concentration of isotype-matched purified IgG. Blots were developed using the enhanced chemiluminescence Western blotting detection system "ECL + Plus" (Amersham Pharmacia Biotech, Arlington Heights, IL) according to manufacturer's recommendations. Quantification of CFH, MAC/C9, and  $\beta$ -actin was accomplished by analyzing the intensity of the bands using Quantity one 4.2.0 (Bio-Rad). Experiment was repeated three times with similar results.

### Alternative Pathway Activity Assay

CFH siRNA ( $n = 5$  mice), scrambled siRNA ( $n = 5$  mice), and PBS ( $n = 5$  mice)-treated animals were sacrificed at day 3 and 5 postlaser treatment. Alternative pathway activity in mouse serum was measured using a modification of the zymosan assay, which measures C3 deposition on zymosan particles.<sup>26,27</sup> In brief, 10  $\mu$ l of mouse serum was incubated with 10<sup>6</sup> activated zymosan particles (Complement Technology) at 37°C for 20 minutes in PBS containing 1% BSA, 10 mmol/L EGTA, and 5 mmol/L MgCl<sub>2</sub>. Particles were then washed and treated with FITC-conjugated goat anti-mouse C3 antibody (MP Biomedicals, Solon, OH) at 4°C for 20 minutes, and surface C3 was analyzed by flow cytometry. Alternative pathway activity was calculated as the % C3 deposition = (Mean % Particle Fluorescence of the sample reaction) – (Mean % Particle Fluorescence of the background).

### Statistical Analysis

Data were analyzed and compared using Student's *t*-test, Mann Whitney test, or analysis of variance and differences were considered statistically significant with  $P < 0.05$ . Data are represented as mean  $\pm$  SE.

## Results

### CFH and MAC Levels During Laser-Induced CNV

C57BL/6 mice were sacrificed at day 1, 3, 5, and 7 postlaser and immunofluorescent staining was performed on RPE-choroid-sclera flat mounts as well as paraffin-embedded serial sections of the laser spots. CFH expression was investigated by RT-PCR and MAC (C9) levels were investigated by Western blot analysis.

### RPE-Choroid-Sclera Flat Mounts

Under confocal microscope, basal (constitutive) expression of CFH was observed on RPE-choroid-sclera tissue harvested from control nonlasered (naïve) mice (Figure 1, A and F). CFH levels in the laser spot decreased significantly ( $P < 0.05$ ) at day 1 postlaser (Figure 1, B and F) compared to naïve mice. On day 3 expression of CFH returned to basal levels (Figure 1, C and F). We observed a dramatic increase in CFH expression in the laser spots at day 5 (102%) and 7 (140%) compared to naïve control (Figure 1, D, E, and F) and these differences were statistically significant ( $P < 0.05$ ; Figure 1F). In naïve animals, extremely low levels of MAC were detected in RPE-choroid-sclera tissue (Figure 1, G and L). Increased MAC deposition (compared to control mice) in the laser spots was observed at all time points studied with maximum levels at day 3 and minimum levels at day 7 postlaser (Figure 1, H–K and L). Negative control images (Figure 1, M–Q) did not show any signal.

### RT-PCR Analysis

CFH mRNA levels in RPE-choroid tissues were reduced at day 1 and 3 postlaser and then returned to the basal level as observed in naïve animals at day 5 postlaser (Figure 1, R and S).

### Western Blot Analysis

MAC protein levels in RPE-choroid tissue increased starting from day 1, reached maximum at day 3 (twofold increase compared to naïve control), and then decreased to the basal level at day 7 postlaser (Figure 1, T and U).

### Paraffin-Embedded Serial Sections

In the naïve mice, strong staining for CFH was detected in RPE cells (Figure 2A). One day after laser treatment we found decrease in CFH levels on RPE cells (Figure 2B) compared to naïve animals (Figure 2A). Intensity of CFH fluorescence in RPE cells increased at day 3 (Figure 2C) to the levels observed in naïve animals with increase at day 5 (Figure 2D) and day 7 (Figure 2E) postlaser treatment. Extremely low levels of MAC were detected on RPE cells in nonlasered animals (Figure 2F). Levels of MAC on RPE cells increased on day 1 (Figure 2G) and 3 (Figure 2H) postlaser. Interestingly, levels of MAC declined at day 5 (Figure 2I) and 7 (Figure 2J) but were still higher to those in naïve mice (Figure 2F). Figure 2K–O represent merged images of CFH, MAC, and DIC. Negative controls (Figure 2, P–T) did not show any signal.

### Effect of CFH Suppression on Laser-Induced CNV

Experiments were performed to explore the effect of ocular CFH inhibition on the incidence and the size of CNV complex as well as on local complement activation. In

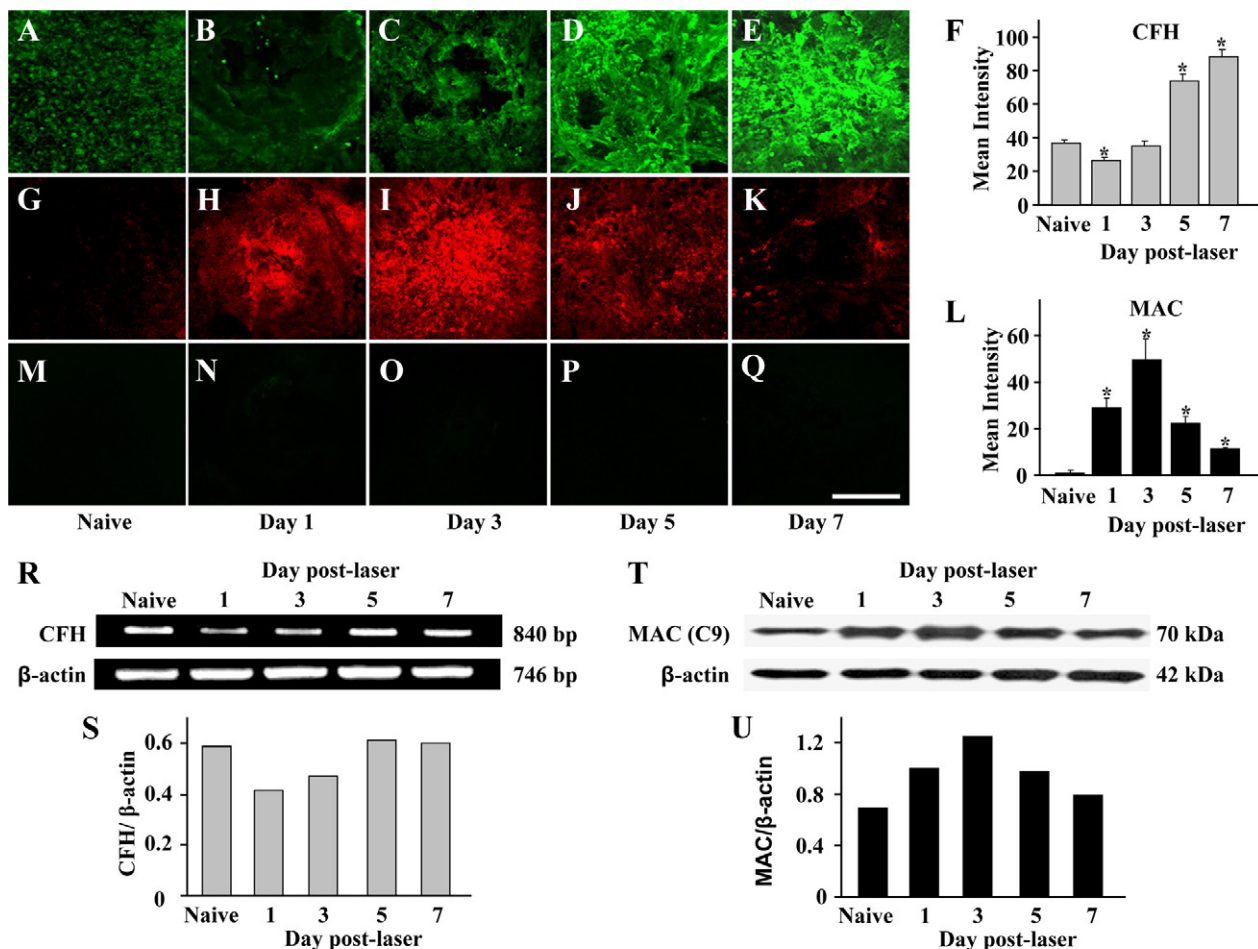


**Figure 1.** Immunohistochemical staining of CFH and MAC in the laser spots during laser-induced CNV. Representative confocal microphotographs of RPE-choroid-scleral flat mounts demonstrate positive signals for CFH (A–E, green) and MAC (G–K, red). Negative control images (M–Q) did not show any signal. Graphs show semiquantitative evaluation of positive fluorescent signals for CFH (F) and MAC (L). R and S: RT-PCR analysis for CFH transcripts in RPE-choroid during laser-induced CNV (R) and quantitation of the analysis (S). T and U: Western blot analysis of MAC in RPE-choroid during laser-induced CNV (T) and quantitation of the analysis (U). Scale bar = 100  $\mu$ m. Data are reported as the mean  $\pm$  SE, \* $P$  < 0.05.

vivo expression of CFH was knock-downed using siRNA directed against CFH gene.

#### Suppression of CFH mRNA and Protein in RPE and Choroid

We first examined whether siRNA directed against CFH can knock-down the expression of gene encoding CFH in RPE and choroid in laser treated mice. Two doses (20 pM and 80 pM) of CFH siRNA mixture were injected separately at the day of laser treatment (day 0), and mice were sacrificed at day 1, 3, 5, and 7 postlaser. Assessment of CFH suppression was done by semiquantitative RT-PCR and semiquantitative Western blot analysis using RPE-choroid tissue. We observed that the subretinal injection of 20 pM and 80 pM (Figure 3, A and B) of CFH siRNA mixture resulted in the inhibition of CFH in a dose-dependent manner with maximum inhibition observed when 80 pM of CFH siRNA was used. Subretinal injection of 80 pM of CFH siRNA mixture resulted in approximately threefold inhibition of CFH transcript (Figure 3, C and D)

and protein (Figure 3, E and F) within RPE and choroid and this effect lasted till day 7 postlaser (Figure 3, C–F).

Similar treatment of laser-treated mice with scrambled siRNA or the vehicle did not affect the levels of CFH mRNA and protein (Figure 3, C–F). siRNA (80 pM) targeted to CFH did not affect the expression of  $\beta$ -actin (Figure 3, C and E). These results demonstrated the specificity of CFH gene suppression by CFH siRNA. Interestingly, subretinal injection of 80 pM of CFH siRNA did not have any effect on the mRNA (Figure 3, G and H) and protein (Figure 3, I and J) levels of CFH in the liver of these animals. Based on these results 80 pM of CFH siRNA was used in subsequent experiments.

#### Effect of CFH siRNA on Systemic Complement Activity

Because only the alternative pathway of complement activation is essential for the development of CNV in the mouse model of laser induced CNV,<sup>15</sup> we investigated the functional activity of the alternative pathway in the

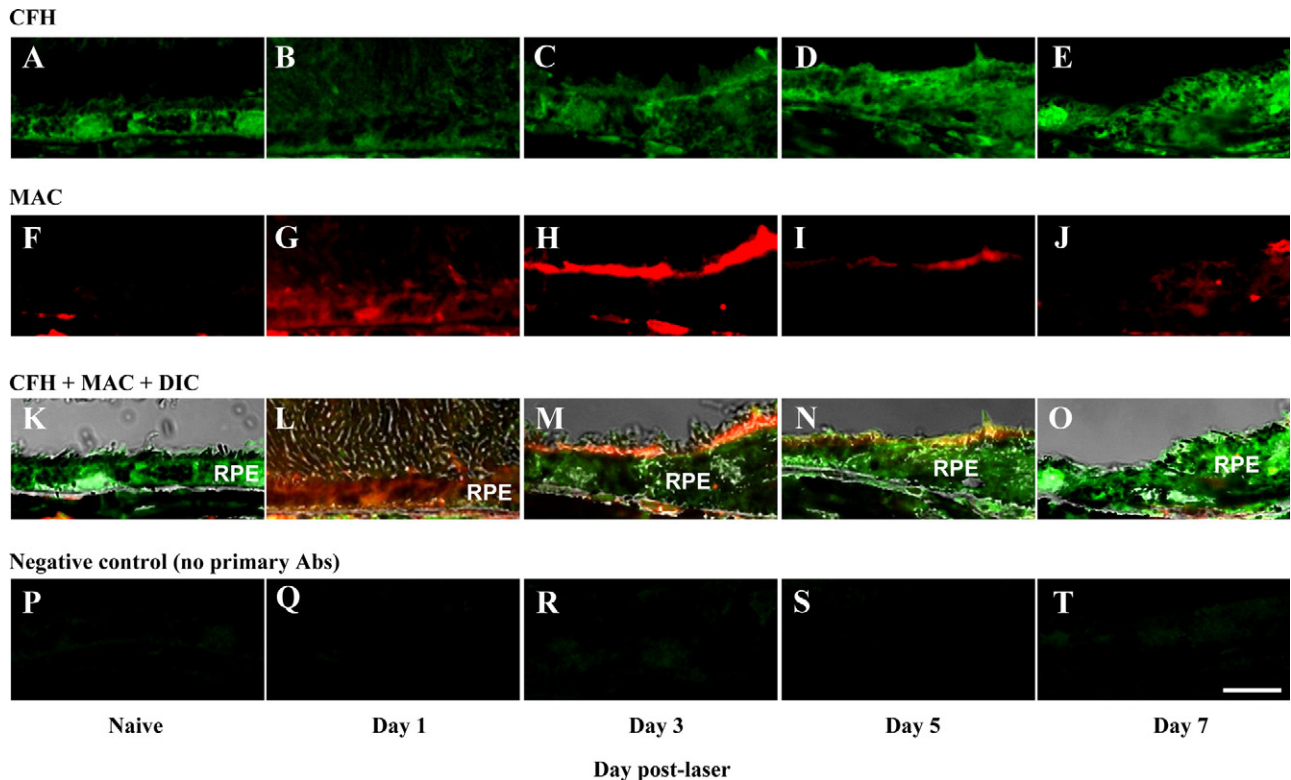


**Figure 2.** Immunohistochemical staining of CFH and MAC in the laser spots during laser-induced CNV. Representative confocal microphotographs (paraffin sections) of laser-injured areas demonstrate positive signals for CFH (A–E, green) and MAC (F–J, red) in RPE cells. Panels K–O represent merged images of CFH, MAC, and DIC. Negative controls (P–T) did not show any signal. Scale bar = 10  $\mu$ m.

serum of mice treated with 80 pM of CFH siRNA. The functional activity of the alternative pathway in CFH siRNA-treated mice was similar to that observed in vehicle and scrambled siRNA-treated mice at day 3 and 5 postlaser (Figure 3K).

#### Localization of CFH siRNA in RPE and Choroid

Experiments were performed to see whether CFH siRNA and control siRNA can be detected in RPE and choroid of the mouse eye after subretinal injection. Animals were lasered and injected with 80 pM of AF488-modified CFH siRNA (CFH AF488) immediately after laser. Serial sections of mouse eyes were analyzed, and no fluorescence was detected in the RPE and choroid of naïve animals that were not injected with CFH AF488 siRNA (Figure 4A). Low green fluorescence detected in choroids capillaries of naïve animals was autofluorescence due to erythrocytes located in capillaries (Figure 4A). At day 1 after injection fluorescent particles appeared inside and outside of RPE cells and in great amount in area of laser injury (Figure 4, B and D). Highest amount of AF488-siRNA was detected at day 3 and 5 and green fluorescence occupied mostly whole cytoplasm of RPE cells, and also was found in the choroid and spot area (Figure 4, C, E, F, and H). At day 7 after injection of AF488-siRNAs green fluorescence became less intense but was still detected in RPE-choroid and spot area (Figure 4, G and I). The localization of CFH siRNA and control siRNA labeled with AF488 in RPE-choroid was

similar (Figure 4, B–I and Supplemental Figure 1, A–H at <http://ajp.amjpathol.org>). Flat mounts from the animals injected with CFH and control AF488 siRNA were also stained for CFH protein. Our results of immunohistochemical staining shown in Figure 4, L–M and Supplemental Figure 1, I and J (at <http://ajp.amjpathol.org>) revealed decreased staining for CFH protein in CFH AF488 siRNA compared to control AF488 siRNA-treated animals. Western blot results also demonstrated that CFH siRNA inhibited expression of CFH in laser spots at day 7 after injection (Figure 4, J, K, and L). Injection of control AF488 siRNA did not have any effect on the levels of CFH protein (Figure 4, J, K, and M). Autofluorescence of tissue (Figure 4N) was eliminated by treating the samples with Sudan Black (Figure 4O). This experiment was repeated three times.

#### Laser-Induced CNV in CFH siRNA-Treated Mice

We next investigated the *in vivo* silencing effect of siRNA targeting the gene for CFH on the development of CNV complex. Animals received a single subretinal injection of vehicle, control (80 pM), or CFH (80 pM) siRNA at day 0 (day of laser) and were sacrificed at day 1, day 3, day 5, and day 7 postlaser. Confocal analysis of RPE-choroid-sclera flat mounts revealed that at day 1 postlaser CNV did not develop in vehicle, control siRNA, and CFH siRNA injected animals (see Supplemental Figure 2, A–C at <http://ajp.amjpathol.org>). Interestingly, at days 3–7 after laser treatment, CFH siRNA-treated mice (Figure 5, D–F)

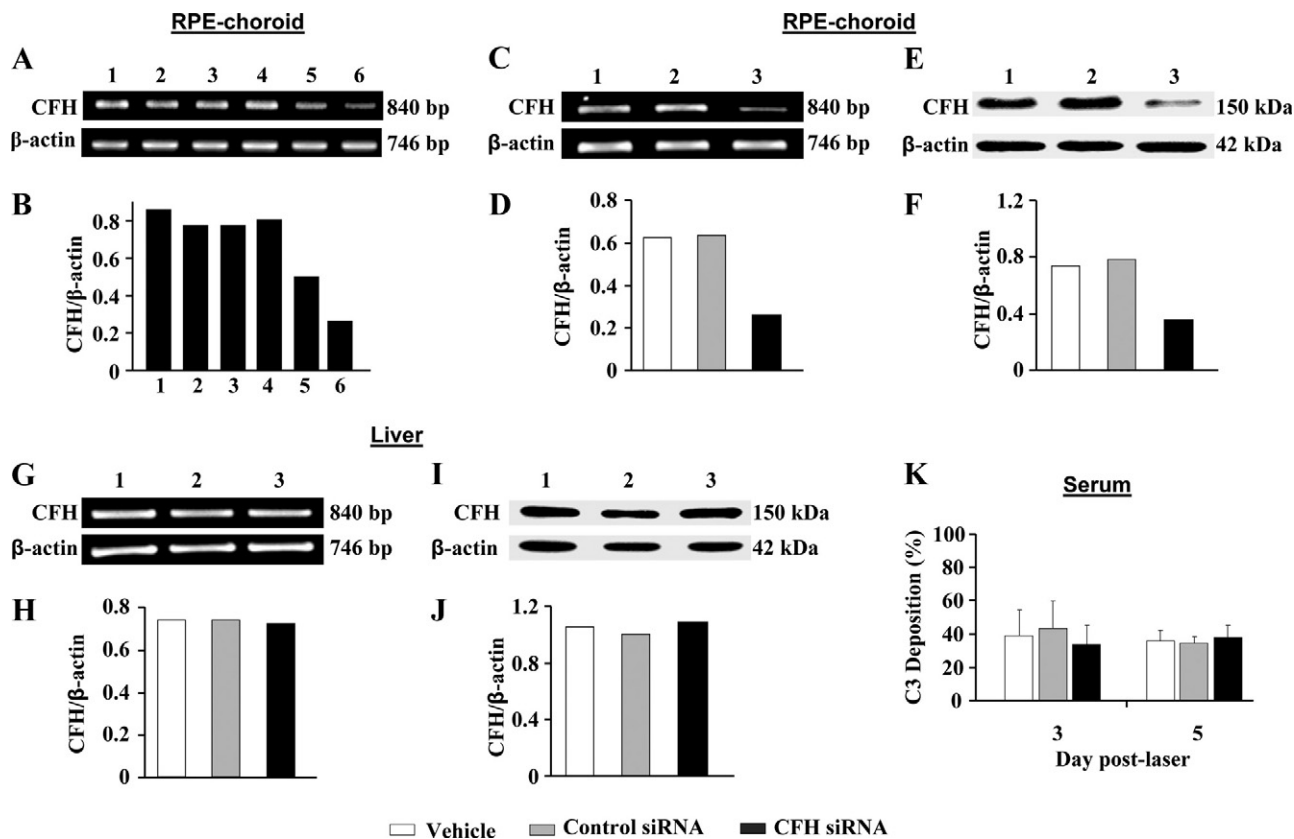


**Figure 3.** **A and B:** Effects of different amounts of siRNA administered subretinally on the expression of CFH transcripts in RPE and choroid. **Lane 1,** Naive, no injection; **lane 2,** vehicle; **lane 3,** 20 pM control siRNA; **lane 4,** 80 pM control siRNA; **lane 5,** 20 pM CFH siRNA; **lane 6,** 80 pM CFH siRNA. **C–J:** siRNA-mediated inhibition of CFH *in vivo*. C57BL/6 mice were injected subretinally with 80 pM CFH siRNA, scrambled siRNA, or vehicle. Total protein and total RNA isolated from RPE and choroid (**C–F**) and liver (**G–J**) were subjected to semiquantitative RT-PCR (**C, D, G, and H**) and Western blot (**E, F, I, and J**) analyses and quantified. **Lane 1,** vehicle; **lane 2,** control siRNA; **lane 3,** CFH siRNA. **K:** Functional activity of the alternative pathway of the complement system in the blood of C57BL/6 mice injected with vehicle, control siRNA, or CFH siRNA. The data are representative of three different experiments.

were more susceptible to laser-induced CNV than vehicle (see Supplemental Figure 2, D–F at <http://ajp.amjpathol.org>) or scrambled siRNA treated mice (Figure 5, A–C), and these differences were statistically significant (Figure 5G;  $P < 0.05$ ). At day 3 postlaser 44% of laser spots were CNV positive in CFH siRNA treated animals compared to 11% CNV positive laser spots in scrambled siRNA treated mice (Table 1). Scrambled siRNA-treated mice (Figure 5A) developed very mild CNV compared to CFH siRNA-treated animals (Figure 5D) at this time point. CFH siRNA treated mice developed more severe CNV compared to control siRNA-treated mice at day 5 (Figure 5, B, E, and G) and day 7 (Figure 5, C, F, and G).

#### Effect CFH siRNA on Local Complement Activation

Formation of MAC was used as a measure of local complement activation, and flat mounts of CNV complex were stained for the presence of MAC. At day 3, 5, and 7, laser spots stained more intensely for MAC in CFH siRNA-treated mice (Figure 6, D–F) compared to vehicle (see Supplemental Figure 3, A–C at <http://ajp.amjpathol.org>) and control siRNA-treated animals (Figure 6, A–C), and these differences were statistically significant (Figure 6G). No staining was observed in CNV complexes stained without the primary antibody (see Supplemental Figure 3, D–F at

<http://ajp.amjpathol.org>). Additionally, RPE-choroid tissue pooled separately from CFH siRNA, control siRNA, and vehicle-injected mice were used in semiquantitative Western blot analysis for MAC. Samples were analyzed on 7.5% SDS-PAGE slab gel under reducing conditions. Increased levels of MAC/C9 protein were detected in CFH siRNA-treated animals compared to vehicle (see Supplemental Figure 3G at <http://ajp.amjpathol.org>) and control siRNA treated mice at day 3, day 5, and day 7 postlaser (Figure 6, H and I).

#### Discussion

AMD is the major cause of irreversible central vision loss among elderly worldwide. Clinically, AMD is classified into two forms, namely “dry” and “wet” AMD. Catastrophic vision loss is more frequently associated with the wet (exudative) form of AMD specifically from the complication of choroidal neovascularization.<sup>2,3</sup> Untreated CNV leads to the loss of central vision in AMD patients and thus has a profound impact on the quality of life. Reports from our as well as other laboratories suggest that complement dysfunction contributes to exudative form of AMD in experimental animals and in humans.<sup>2,4,5,10,11</sup>

Rodent model of CNV induced by laser photocoagulation has been extensively studied in our laborat-

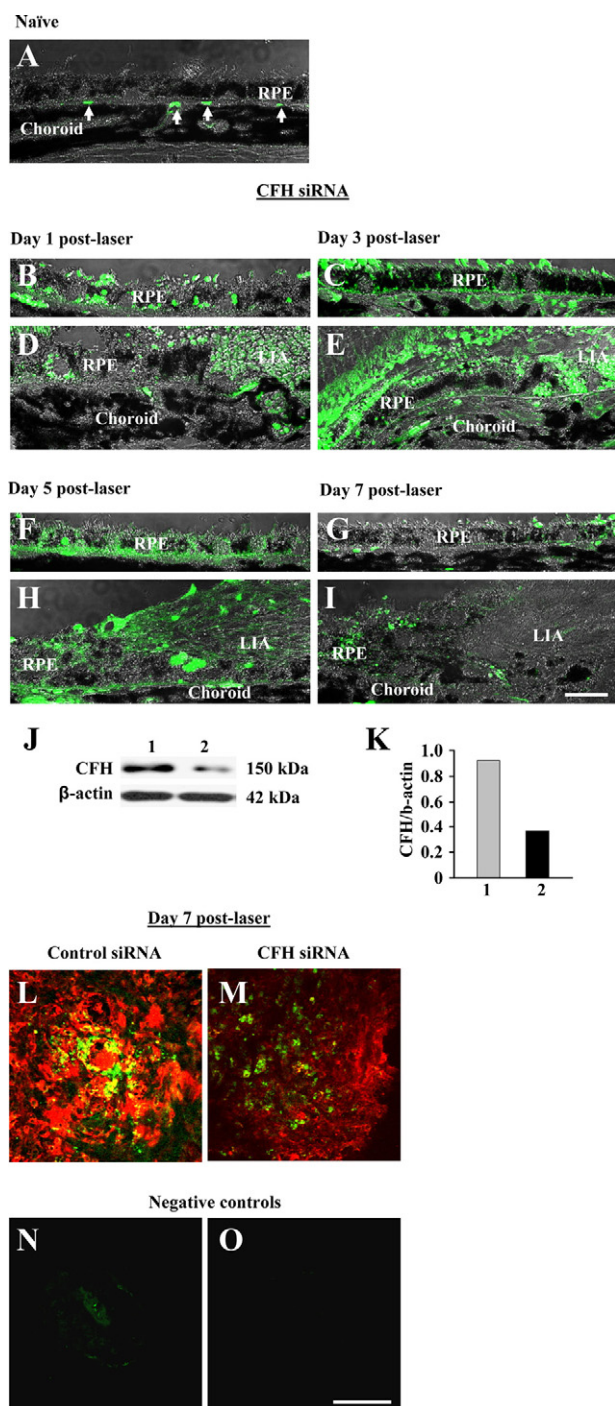


**Figure 4.** Localization of CFH siRNA labeled with AF488 in RPE and choroid of C57BL/6 mice after subretinal administration. No green fluorescence was detected in RPE and choroid of naïve mice (**A**). Erythrocytes located in choroid capillaries had green autofluorescence (**arrow**). Confocal microphotographs of paraffin sections show CFH siRNA labeled with AF488 in green, overlapping with differential interference contrast images of RPE-choroid (**B–I**) during laser-induced CNV. Intense green signal was found in RPE cells, choroid, and laser-injured areas (LIA). **J** and **K**: Western blot (**J**) analysis of CFH expression in RPE-choroid after subretinal injection of control siRNA labeled with AF488 (**lane 1**) and CFH siRNA labeled with AF488 (**lane 2**) and its quantification (**K**). Immunohistochemical staining of RPE-choroid flat mounts for CFH (red color) after subretinal injection of control siRNA labeled with AF488 (green color, **L**) and CFH siRNA labeled with AF488 (green color, **M**) investigated on day 7 postinjury. Autofluorescence of tissue (**N**) was eliminated by treating the samples with Sudan Black (**O**). Scale bar: 20  $\mu\text{m}$  (**A–I**); 100  $\mu\text{m}$  (**L–O**).

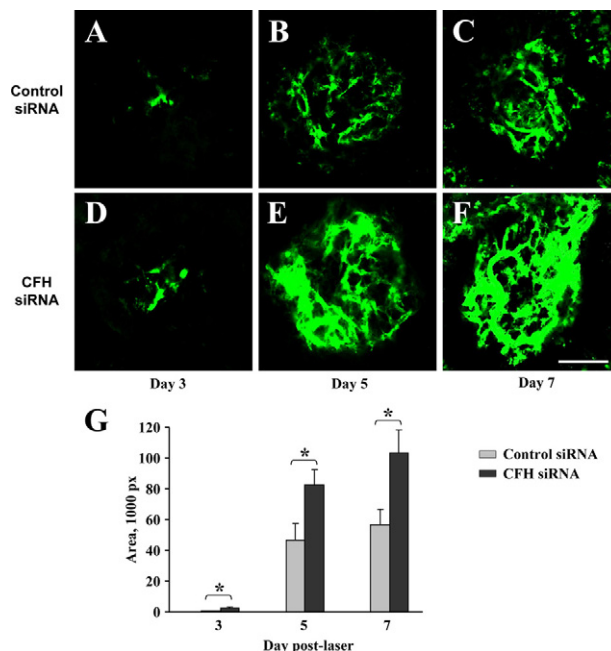


**Figure 5.** Effects of CFH siRNA administration on the size of the CNV complex. Representative confocal microphotographs of RPE-choroid-scleral flat mounts with FITC-dextran-perfused vessels (green) from control siRNA (**A–C**) and CFH siRNA (**D–F**) injected mice sacrificed at day three (**A** and **D**), day five (**B** and **E**), and day seven (**C** and **F**) are shown. Quantification of the images is shown in **G**. Scale bar = 100  $\mu\text{m}$ . Data are reported as the mean  $\pm$  SE, \* $P < 0.05$ .

ory.<sup>4,5,14,15,28–33</sup> Using this model our previous studies have demonstrated precisely the role played by complement; specifically the alternative pathway of complement activation in the development of wet-AMD.<sup>4,15,29,31</sup> In addition, our studies described the first direct role of complement activation product—MAC in the mouse model of laser-induced CNV. We have established that generation and the release of angiogenic growth factors in laser-induced CNV is dependent on MAC formation.<sup>4,15,29,31</sup> Thus, data from our laboratory clearly implicate MAC formed via the alternative pathway activation as a major mediator of CNV in the murine model.<sup>4,15,29,31</sup> Interestingly, we also observed that the levels (both transcripts and protein) of CFH in RPE and choroid were markedly reduced during the growth of CNV complex in mice.<sup>15</sup> In the present study we asked the question whether CFH locally present in RPE and choroid regulates the development of CNV in C57BL/6 mice and explored the underlying mechanisms.

CFH, a 155-kDa glycoprotein, exclusively regulates the function of the alternative complement pathway<sup>16,17</sup> and a common variant (Tyr402His) of CFH gene is associated with AMD susceptibility in humans in the United States as well as several populations worldwide.<sup>2,6–8,12,16,17,20,21,34,35</sup> It has been suggested that Y420H polymorphism of CFH leads to impaired complement regulation, and the risk variant CFH Y420H is inefficient in regulating the complement system.<sup>20,36</sup>

Using semiquantitative immunohistochemistry we observed that MAC was expressed constitutively in RPE and choroid of naïve mouse eyes. In 2000, we reported

**Table 1.** Laser-Induced CNV in CFH siRNA-Treated Mice on Day 3 Post-Laser

Treatment	Number of mice	Laser spots/eye	Total spots	CNV-positive spots (%)	CNV-negative spots (%)
Control siRNA	15	3	45	5 (11)	40 (89)
CFH siRNA	15	3	45	20 (44)	25 (56)

the presence of MAC in the normal rat eye as a result of chronic low level complement activation.<sup>37</sup> In the present study we noted that both mRNA and protein for CFH were present in RPE-choroid tissue harvested from the eyes of naïve mice. The presence of CFH transcripts and protein described in our current study suggests that CFH is locally produced by RPE and choroid. Although liver is the major site of CFH synthesis, extrahepatic production

of CFH was observed in a variety of cell types.<sup>16,38</sup> In a previous report, CFH expression was detected in several tissues of normal human and mouse eyes.<sup>12,18,19</sup>

The expression pattern of CFH and MAC during laser-induced CNV was studied using IHC of flat-mount and paraffin embedded sections, Western blot, and RT-PCR analysis. MAC levels were up-regulated in RPE during the initiation of growth (ie, day 1 and 3) of the CNV complex. Increased complement activation during the growth phase of laser-induced CNV<sup>5,14</sup> will lead to increased MAC levels at day 1 and 3 postlaser observed in our current study. Amount of MAC decreased during the maturation phase (ie, day 5 and 7) of CNV suggesting thereby that ocular cells protect themselves by down-regulating complement activation leading to reduced MAC deposition.<sup>5,14</sup> Higher deposition of MAC (C5b-9) was found in Bruch's membrane, intercapillary pillars, and within drusen<sup>12,18</sup> in patients with AMD compared to control subjects.

In the present study we observed that CFH levels decreased significantly in the early phase of CNV (day 1 postlaser) and then increased in the laser spot on days 5 and 7 postlaser. Decreased levels of CFH at day 1 postlaser may be due to its reduced synthesis resulting from cell damage caused by laser-treatment. A combination of several factors may explain the increase in the levels of CFH in these tissues at day 5 and 7 postlaser. First, our present results suggest that CFH is produced locally in the RPE and the choroid. Secondly, CFH produced by the liver circulates through out the body via blood and blood-derived CFH may also contribute to ocular CFH pool. Circulating blood cells containing CFH<sup>16,38</sup> may also contribute to CFH levels; it is known that blood cells and bone marrow cells express CFH.<sup>16,38</sup> In previous studies, CFH was observed in human and mouse choroidal vessels.<sup>12,39</sup> CFH was found in drusen, subretinal space, and around choroid capillaries.<sup>12,18,20,40</sup>

The importance of CFH in regulating local (ie, ocular) complement activation and choroidal vessel growth was confirmed by using CFH siRNA. siRNA directed against complement proteins have provided valuable information in efforts to understand the *in vivo* role of complement in animals models of ocular diseases.<sup>15,41</sup> We examined the disease course and severity in CFH siRNA-treated mice and observed that mice in which CFH gene was knocked-down in the eye developed the CNV complex early in the disease process and more severe CNV at later time points compared to control siRNA-treated animals. C9/MAC deposition levels were significantly increased in the CFH siRNA-treated group. Thus, our results have demonstrated for the first time that local suppression of CFH gene exacerbates laser-induced CNV in mice by allowing unregulated MAC deposition. VEGF has been documented to play an important role in

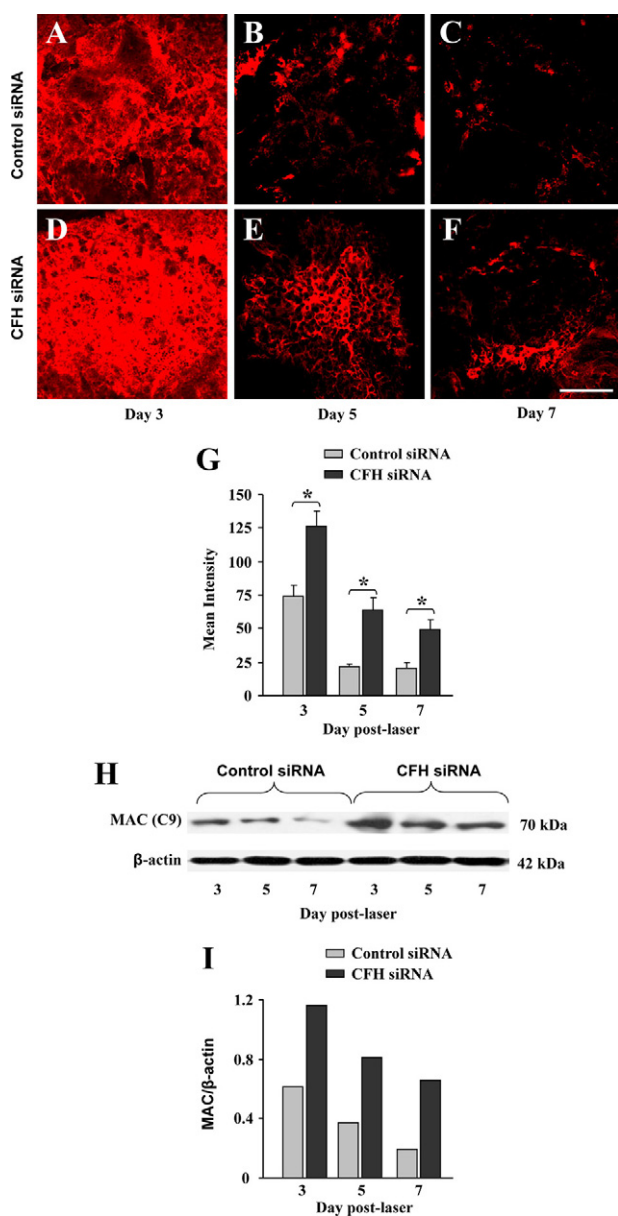


**Figure 6.** Effects of CFH siRNA (D–G) and control siRNA (A–C and G) on MAC deposition in laser spots. Semiquantitative Western blot analysis of RPE-choroid tissue for MAC/C9 during laser-induced CNV (H) and the quantification of the analysis (I). Scale bar = 100 μm. Data are reported as the mean ± SE, \*P < 0.05.

the development of CNV associated with wet AMD,<sup>2,3</sup> and MAC has been reported to release growth factors including VEGF from cells.<sup>4,15,31</sup> In our study, the subretinal injection of CFH siRNA had no effect on CFH expression in the liver. These results also suggest that the decrease of CFH mRNA and protein in RPE-choroid after subretinal injection of CFH siRNA was due to the suppression CFH synthesis in the eye. Importantly, the subretinal injection of CFH siRNA did not affect the functional activity of the alternative pathway in the blood. It is possible that systemic CFH will also play a role and inhibition of systemic CFH along with ocular CFH will further worsen the laser-induced CNV in mice. However, the effect of systemic CFH inhibition on laser-induced CNV was not explored in the present study.

Recently it was reported that the area of laser-induced CNV was significantly larger in aged mice with homozygous CFH deficiency compared to their wild-type (WT) controls.<sup>42</sup> Reduced perfusion of CNV in these CFH KO mice may relate to perfusion effect of CFH inhibition.<sup>42</sup> In mouse model of laser-induced CNV intravenous (via the tail vein) administration of CR2-FH has been reported to reduce CNV size in C57BL/6 mice.<sup>43</sup> CR2-FH is a recombinant complement inhibitor that contains N terminus of mouse CFH linked to complement receptor 2 (CR2). In another report, intraperitoneally injected Thioredoxin-1 was shown to interact with CFH, regulate complement activation, and inhibit laser-induced CNV in C57BL/6 mice.<sup>44</sup> However, local regulation of complement activation as demonstrated by our results reported here has several advantages over systemic complement inhibition reported in other studies.<sup>43,44</sup> This is because local complement inhibition does not have the possible untoward complications associated with systemic complement inhibition resulting from intravenous or intraperitoneal injections. Systemic complement system that plays a crucial role in host response to infection and immune complex catabolism as well as required to facilitate tissue healing will remain intact, and its function will not be hindered if the complement system is inhibited locally.

In conclusion, our results demonstrate that CFH expressed in RPE and choroid is instrumental in regulating the alternative pathway of complement cascade and MAC formation that is essential for the development of CNV. Our results further suggest that ocular inhibition of complement by local administration of recombinant CFH may provide better treatment for AMD.

## References

- Friedman DS, O'Colmain BJ, Muñoz B, Tomany SC, McCarty C, de Jong PT, Nemesure B, Mitchell P, Kempen J, Eye Diseases Prevalence Research Group: Prevalence of age-related macular degeneration in the United States. *Arch Ophthalmol* 2004, 122:564–572
- Coleman HR, Chan CC, Ferris 3rd FL, Chew EY: Age-related macular degeneration. *Lancet* 2008, 372:1835–1845
- Campochiaro PA: Retinal and choroidal neovascularization. *J Cell Physiol* 2000, 184:301–310
- Bora PS, Sohn JH, Cruz JM, Jha P, Nishihori H, Wang Y, Kaliappan S, Kaplan HJ, Bora NS: Role of complement and complement membrane attack complex in laser-induced choroidal neovascularization. *J Immunol* 2005, 174:491–497
- Jha P, Bora PS, Bora NS: The role of complement system in ocular diseases including uveitis and macular degeneration. *Mol Immunol* 2007, 44:3901–3908
- Haddad S, Chen CA, Santangelo SL, Seddon JM: The genetics of age-related macular degeneration: a review of progress to date. *Surv Ophthalmol* 2006, 51:316–363
- Donoso LA, Kim D, Frost A, Callahan A, Hageman G: The role of inflammation in the pathogenesis of age-related macular degeneration. *Surv Ophthalmol* 2006, 51:137–152
- Gehrs KM, Anderson DH, Johnson LV, Hageman GS: Age-related macular degeneration-emerging pathogenetic and therapeutic concepts. *Ann Med* 2006, 38:450–471
- Miller H, Miller B, Ishibashi T, Ryan SJ: Pathogenesis of laser-induced choroidal subretinal neovascularization. *Invest Ophthalmol Vis Sci* 1990, 31:899–908
- Meri S: Loss of self-control in the complement system and innate autoreactivity. *Ann NY Acad Sci* 2007, 1109:93–105
- Nozaki M, Raisier BJ, Sakurai E, Sarma JV, Barnum SR, Lambris JD, Chen Y, Zhang K, Ambati BK, Baffi JZ, Ambati J: Drusen complement component C3a and C5a promote choroidal neovascularization. *Proc Natl Acad Sci USA* 2006, 103:2328–2333
- Klein RJ, Zeiss C, Chew EY, Tsai JY, Sackler RS, Haynes C, Henning AK, SanGiovanni JP, Mane SM, Mayne ST, Bracken MB, Ferris FL, Ott J, Barnstable C, Hoh J: Complement factor H polymorphism in age-related macular degeneration. *Science* 2005, 308:385–389
- Scholl HP, Charbel Issa P, Walier M, Janzer S, Pollok-Kopp B, Börncke F, Fritsche LG, Chong NV, Fimmers R, Wienker T, Holz FG, Weber BH, Oppermann M: Systemic complement activation in age-related macular degeneration. *PLoS ONE* 2008, 3:e2593
- Bora NS, Jha P, Bora PS: The role of complement in ocular pathology. *Semin Immunopathol* 2008, 30:85–95
- Bora NS, Kaliappan S, Jha P, Xu Q, Sohn JH, Dhulakhandi DB, Kaplan HJ, Bora PS: Complement activation via alternative pathway is critical in the development of laser-induced choroidal neovascularization: role of factor B and factor H. *J Immunol* 2006, 177:1872–1878
- Rodriguez de Cordoba S, Esparza-Gordillo J, Goicoechea de Jorge E, Lopez-Trascasa M, Sanchez-Corral P: The human complement factor H: functional roles, genetic variations and disease associations. *Mol Immunol* 2004, 41:355–367
- Zipfel PF, Hallström T, Hammerschmidt S, Skerka C: The complement fitness factor H: role in human diseases and for immune escape of pathogens, like pneumococci. *Vaccine* 2008, 30:167–174
- Hageman GS, Anderson DH, Johnson LV, Hancox LS, Taiber AJ, Hardisty LI, Hageman JL, Stockman HA, Borchardt JD, Gehrs KM, Smith RJ, Silvestri G, Russell SR, Klaver CC, Barbazzetto I, Chang S, Yannuzzi LA, Barile GR, Merriam JC, Smith RT, Olsh AK, Bergeron J, Zernant J, Merriam JE, Gold B, Dean M, Allikmets R: A common haplotype in the complement regulatory gene factor H (HF1/CFH) predisposes individuals to age-related macular degeneration. *Proc Natl Acad Sci USA* 2005, 102:227–7232
- Mandal MN, Ayyagari R: Complement factor H: spatial and temporal expression and localization in the eye. *Invest Ophthalmol Vis Sci* 2006, 47:4091–4097
- Skerka C, Lauer N, Weinberger AA, Keilhauer CN, Sühnel J, Smith R, Schlötzer-Schrehardt U, Fritsche L, Heinen S, Hartmann A, Weber BH, Zipfel PF: Defective complement control of factor H (Y402H) and FHL-1 in age-related macular degeneration. *Mol Immunol* 2007, 44:3398–3406
- Cook HL, Patel PJ, Tufail A: Age-related macular degeneration: diagnosis and management. *Br Med Bull* 2008, 85:127–149
- Edelman JL, Castro MR: Quantitative image analysis of laser-induced choroidal neovascularization in rat. *Exp Eye Res* 2000, 71:523–533
- Robertson D, Savage K, Reis-Filho JS, Isacke CM: Multiple immunofluorescence labelling of formalin-fixed paraffin-embedded (FFPE) tissue. *BMC Cell Biol* 2008, 9:13–22
- Viegas MS, Martins TC, Seco F, do Carmo A: An improved and cost-effective methodology for the reduction of autofluorescence in direct immunofluorescence studies on formalin-fixed paraffin-embedded tissues. *Eur J Histochem* 2007, 51:59–66
- Vik DP, Keeney JB, Munoz-Canoves P, Chaplin DD, Tack BF: Structure of the murine complement factor H gene. *J Biol Chem* 1988, 263:16720–17624
- Huang Y, Qiao F, Atkinson C, Holers VM, Tomlinson S: A Novel

- targeted inhibitor of the alternative pathway of complement and its therapeutic application in ischemia/reperfusion injury. *J Immunol* 2008, 181:8068–8076
27. Clark A, Weymann A, Hartman E, Turmelle Y, Carroll M, Thurman JM, Holers VM, Hourcade DE, Rudnick DA: Evidence for non-traditional activation of complement factor C3 during murine liver regeneration. *Mol Immunol* 2008, 45:3125–3132
  28. Lyzogubov VV, Tytarenko RG, Thotakura S, Viswanathan T, Bora NS, Bora PS: Inhibition of new vessel growth in mouse model of laser-induced choroidal neovascularization by adiponectin peptide II. *Cell Biol Int* 2009, 33:765–771
  29. Kaliappan S, Jha P, Lyzogubov VV, Tytarenko RG, Bora NS, Bora PS: Alcohol and nicotine consumption exacerbates choroidal neovascularization by modulating the regulation of complement system. *FEBS Lett* 2008, 582:3451–3458
  30. Bora PS, Kaliappan S, Lyzogubov VV, Tytarenko RG, Thotakura S, Viswanathan T, Bora NS: Expression of adiponectin in choroidal tissue and inhibition of laser induced choroidal neovascularization by adiponectin. *FEBS Lett* 2007, 581:1977–1982
  31. Bora NS, Kaliappan S, Jha P, Xu Q, Sivasankar B, Harris CL, Morgan BP, Bora PS: CD59, a complement regulatory protein, controls choroidal neovascularization in a mouse model of wet-type age-related macular degeneration. *J Immunol* 2007, 178:1783–1790
  32. Bora PS, Kaliappan S, Xu Q, Kumar S, Wang Y, Kaplan HJ, Bora NS: Alcohol linked to enhanced angiogenesis in rat model of choroidal neovascularization. *FEBS J* 2006, 273:1403–1414
  33. Bora PS, Hu Z, Tezel TH, Sohn JH, Kang SG, Cruz JM, Bora NS, Garen A, Kaplan HJ: Immunotherapy for choroidal neovascularization in a laser-induced mouse model simulating exudative (wet) macular degeneration. *Proc Natl Acad Sci USA* 2003, 100:2679–2684
  34. Edwards AO, Ritter R, Abel KJ, Manning A, Panhuysen C, Farrer LA: Complement factor H polymorphism and age-related macular degeneration. *Science* 2005, 308:421–424
  35. Gu J, Paeur GJ, Yue X, Narendra U, Sturgill GM, Bena J, Gu X, Peachey NS, Salomon RG, Hagstrom SA, Crabb JW, Clinical Genomic And Proteomic Study Group: Assessing susceptibility to age-related macular degeneration with proteomic and genomic biomarkers. *Mol Cell Proteomics* 2009, 8:1338–1349
  36. Laine M, Jarva H, Seitonen S, Haapasalo K, Lehtinen MJ, Lindeman N, Anderson DH, Johnson PT, Järvelä I, Jokiranta TS, Hageman GS, Immonen I, Meri S: Y402H polymorphism of complement factor H affects binding affinity to C-reactive protein. *J Immunol* 2007, 178:3831–3836
  37. Sohn JH, Kaplan HJ, Suk HJ, Bora PS, Bora NS: Chronic low level complement activation within the eye is controlled by intraocular complement regulatory proteins. *Invest Ophthalmol Vis Sci* 2000, 41:3492–3502
  38. Schlaf G, Demberg T, Beisel N, Schieferdecker HL, Götze O: Expression and regulation of complement factors H and I in rat and human cells: some critical notes. *Mol Immunol* 2001, 38:231–239
  39. Chen M, Forrester JV, Xu H: Synthesis of complement factor H by retinal pigment epithelial cells is down-regulated by oxidized photoreceptor outer segments. *Exp Eye Res* 2007, 84:635–645
  40. Lommatzsch A, Hermans P, Weber B, Pauleikhoff D: Complement factor H variant Y402H and basal laminar deposits in exudative age-related macular degeneration. *Graefes Arch Clin Exp Ophthalmol* 2007, 245:1713–1716
  41. Jha P, Sohn JH, Xu Q, Wang Y, Kaplan HJ, Bora PS, Bora NS: Suppression of complement regulatory proteins (CRPs) exacerbates experimental autoimmune anterior uveitis (EAAU). *J Immunol* 2006, 176:7221–7231
  42. Lundh von Leithner P, Kam JH, Bainbridge J, Catchpole I, Gough G, Coffey P, Jeffery G: Complement factor h is critical in the maintenance of retinal perfusion. *Am J Pathol* 2009, 175:412–421
  43. Rohrer B, Long Q, Coughlin B, Wilson RB, Huang Y, Qiao F, Tang PH, Kunchithapautham K, Gilkeson GS, Tomlinson S: A targeted inhibitor of the alternative complement pathway reduces angiogenesis in a mouse model of age-related macular degeneration. *Invest Ophthalmol Vis Sci* 2009, 50:3056–3064
  44. Inomata Y, Tanihara H, Tanito M, Okuyama H, Hoshino Y, Kinumi T, Kawaji T, Kondo N, Yodoi J, Nakamura H: Suppression of choroidal neovascularization by thioredoxin-1 via interaction with complement factor H. *Invest Ophthalmol Vis Sci* 2008, 49:5118–5125